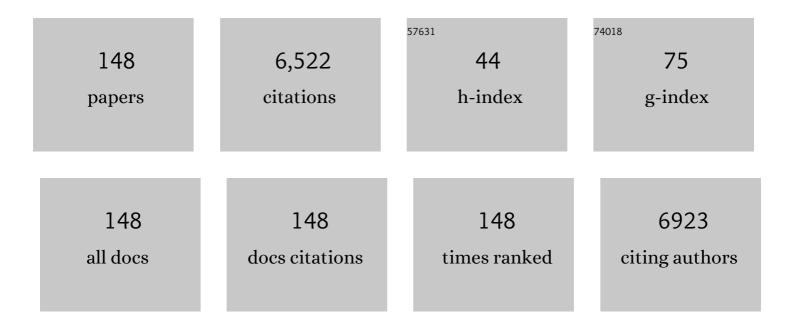
BjÃ, rn T Stokke

List of Publications by Year in descending order

Source: https://exaly.com/author-pdf/8613400/publications.pdf Version: 2024-02-01



RIÃ DNI T STORVE

#	Article	IF	CITATIONS
1	Interrelation between swelling, mechanical constraints and reaction–diffusion processes in molecular responsive hydrogels. Soft Matter, 2022, 18, 1510-1524.	1.2	3
2	Signal Amplification of a Gravimetric Glucose Biosensor Based on the Concanavalin A–Dextran Affinity Assay. IEEE Sensors Journal, 2021, 21, 4391-4404.	2.4	3
3	Fabrication of monodisperse alginate microgel beads by microfluidic picoinjection: a chelate free approach. Lab on A Chip, 2021, 21, 2232-2243.	3.1	25
4	Characterization of Mixing Performance Induced by Double Curved Passive Mixing Structures in Microfluidic Channels. Micromachines, 2021, 12, 556.	1.4	4
5	On the Determination of Mechanical Properties of Aqueous Microgels—Towards High-Throughput Characterization. Gels, 2021, 7, 64.	2.1	6
6	A Titratable Cell Lysis-on-Demand System for Droplet-Compartmentalized Ultrahigh-Throughput Screening in Functional Metagenomics and Directed Evolution. ACS Synthetic Biology, 2021, 10, 1882-1894.	1.9	4
7	DNA Aptamer Functionalized Hydrogels for Interferometric Fiber-Optic Based Continuous Monitoring of Potassium Ions. Biosensors, 2021, 11, 266.	2.3	5
8	Toehold Length of Target ssDNA Affects Its Reaction-Diffusion Behavior in DNA-Responsive DNA- <i>co</i> -Acrylamide Hydrogels. Biomacromolecules, 2020, 21, 1687-1699.	2.6	7
9	Donnan Contribution and Specific Ion Effects in Swelling of Cationic Hydrogels are Additive: Combined High-Resolution Experiments and Finite Element Modeling. Gels, 2020, 6, 31.	2.1	11
10	Impact of Silanization Parameters and Antibody Immobilization Strategy on Binding Capacity of Photonic Ring Resonators. Sensors, 2020, 20, 3163.	2.1	16
11	Morpholino Target Molecular Properties Affect the Swelling Process of Oligomorpholino-Functionalized Responsive Hydrogels. Polymers, 2020, 12, 268.	2.0	1
12	Myeloma-derived extracellular vesicles mediate HGF/c-Met signaling in osteoblast-like cells. Experimental Cell Research, 2019, 383, 111490.	1.2	10
13	The Characterisation and Quantification of Immobilised Concanavalin A on Quartz Surfaces Based on The Competitive Binding to Glucose and Fluorescent Labelled Dextran. Applied Sciences (Switzerland), 2019, 9, 318.	1.3	8
14	Nanoparticle-Hydrogel Composites: From Molecular Interactions to Macroscopic Behavior. Polymers, 2019, 11, 275.	2.0	142
15	Tn and STn are members of a family of carbohydrate tumor antigens that possess carbohydrate–carbohydrate interactions. Glycobiology, 2018, 28, 437-442.	1.3	16
16	Self-Coacervation of a Silk-Like Protein and Its Use As an Adhesive for Cellulosic Materials. ACS Macro Letters, 2018, 7, 1120-1125.	2.3	29
17	In vitro single-cell dissection revealing the interior structure of cable bacteria. Proceedings of the National Academy of Sciences of the United States of America, 2018, 115, 8517-8522.	3.3	45
18	Polymer sequencing by molecular machines: a framework for predicting the resolving power of a sliding contact force spectroscopy sequencing method. Nanoscale, 2017, 9, 15089-15097.	2.8	1

#	Article	IF	CITATIONS
19	Interactions between the breast cancer-associated MUC1 mucins and C-type lectin characterized by optical tweezers. PLoS ONE, 2017, 12, e0175323.	1.1	12
20	Microarrays for the study of compartmentalized microorganisms in alginate microbeads and (W/O/W) double emulsions. RSC Advances, 2016, 6, 114830-114842.	1.7	10
21	Sliding Contact Dynamic Force Spectroscopy Method for Interrogating Slowly Forming Polymer Cross-Links. Langmuir, 2016, 32, 12814-12822.	1.6	6
22	Recovering fluorophore concentration profiles from confocal images near lateral refractive index step changes. Journal of Biomedical Optics, 2016, 21, 126014.	1.4	4
23	Effects of added oligoguluronate on mechanical properties of Ca – alginate – oligoguluronate hydrogels depend on chain length of the alginate. Carbohydrate Polymers, 2016, 147, 234-242.	5.1	10
24	Single molecule investigation of the onset and minimum size of the calcium-mediated junction zone in alginate. Carbohydrate Polymers, 2016, 148, 52-60.	5.1	28
25	Local structure of Ca 2+ induced hydrogels of alginate–oligoguluronate blends determined by small-angle-X-ray scattering. Carbohydrate Polymers, 2016, 152, 532-540.	5.1	20
26	Bioresponsive DNA-co-polymer hydrogels for fabrication of sensors. Current Opinion in Colloid and Interface Science, 2016, 26, 1-8.	3.4	21
27	Versatile, cell and chip friendly method to gel alginate in microfluidic devices. Lab on A Chip, 2016, 16, 3718-3727.	3.1	63
28	Nanoindentation and finite element modelling of chitosan–alginate multilayer coated hydrogels. Soft Matter, 2016, 12, 7338-7349.	1.2	11
29	Competitive ligand exchange of crosslinking ions for ionotropic hydrogel formation. Journal of Materials Chemistry B, 2016, 4, 6175-6182.	2.9	38
30	Interactions of mucins with the Tn or Sialyl Tn cancer antigens including MUC1 are due to GalNAc–GalNAc interactions. Glycobiology, 2016, 26, 1338-1350.	1.3	8
31	Swelling Dynamics of a DNA-Polymer Hybrid Hydrogel Prepared Using Polyethylene Glycol as a Porogen. Gels, 2015, 1, 219-234.	2.1	9
32	<scp>CD14</scp> , <scp>TLR4</scp> and <scp>TRAM</scp> Show Different Trafficking Dynamics During <scp>LPS</scp> Stimulation. Traffic, 2015, 16, 677-690.	1.3	35
33	Direct Determination of Chitosan–Mucin Interactions Using a Single-Molecule Strategy: Comparison to Alginate–Mucin Interactions. Polymers, 2015, 7, 161-185.	2.0	32
34	Delaying cluster growth of ionotropic induced alginate gelation by oligoguluronate. Carbohydrate Polymers, 2015, 133, 126-134.	5.1	7
35	Novel imaging technologies for characterization of microbial extracellular polysaccharides. Frontiers in Microbiology, 2015, 06, 525.	1.5	11
36	Single molecule study of heterotypic interactions between mucins possessing the Tn cancer antigen. Glycobiology, 2015, 25, 524-534.	1.3	7

#	Article	IF	CITATIONS
37	Energy Landscape of Alginate-Epimerase Interactions Assessed by Optical Tweezers and Atomic Force Microscopy. PLoS ONE, 2015, 10, e0141237.	1.1	7
38	Polyelectrolyte and antipolyelectrolyte effects in swelling of polyampholyte and polyzwitterionic charge balanced and charge offset hydrogels. European Polymer Journal, 2014, 53, 65-74.	2.6	47
39	Structure–Function Relationships in Glycopolymers: Effects of Residue Sequences, Duplex, and Triplex Organization. Biopolymers, 2013, 99, 757-771.	1.2	11
40	The relation of apple texture with cell wall nanostructure studied using an atomic force microscope. Carbohydrate Polymers, 2013, 92, 128-137.	5.1	66
41	PEGylated chitosan complexes DNA while improving polyplex colloidal stability and gene transfection efficiency. Carbohydrate Polymers, 2013, 94, 436-443.	5.1	25
42	Higher order structures of a bioactive, water-soluble (1→3)-β-d-glucan derived from Saccharomyces cerevisiae. Carbohydrate Polymers, 2013, 92, 1026-1032.	5.1	14
43	Swelling of a hemi-ellipsoidal ionic hydrogel for determination of material properties of deposited thin polymer films: an inverse finite element approach. Soft Matter, 2013, 9, 5815.	1.2	9
44	Evidence for Age-Dependent <i>in Vivo</i> Conformational Rearrangement within AÎ ² Amyloid Deposits. ACS Chemical Biology, 2013, 8, 1128-1133.	1.6	93
45	Cyclodextrin triggered dimensional changes of polysaccharide nanogel integrated hydrogels at nanometer resolution. Soft Matter, 2013, 9, 5178.	1.2	10
46	High resolution interferometry as a tool for characterization of swelling of weakly charged hydrogels subjected to amphiphile and cyclodextrin exposure. Journal of Colloid and Interface Science, 2013, 390, 282-290.	5.0	5
47	Nanoscopic and Photonic Ultrastructural Characterization of Two Distinct Insulin Amyloid States. International Journal of Molecular Sciences, 2012, 13, 1461-1480.	1.8	10
48	Impregnation of weakly charged anionic microhydrogels with cationic polyelectrolytes and their swelling properties monitored by a high resolution interferometric technique. Transformation from a polyelectrolyte to polyampholyte hydrogel. European Polymer Journal, 2012, 48, 1949-1959.	2.6	10
49	Oligoguluronate induced competitive displacement of mucin–alginate interactions: relevance for mucolytic function. Soft Matter, 2012, 8, 8413.	1.2	28
50	Enhanced Self-Association of Mucins Possessing the T and Tn Carbohydrate Cancer Antigens at the Single-Molecule Level. Biomacromolecules, 2012, 13, 1400-1409.	2.6	18
51	Direct measurement of the interaction force between immunostimulatory CpG–DNA and TLR9 fusion protein. Journal of Molecular Recognition, 2012, 25, 74-81.	1.1	5
52	Isothermal titration calorimetry study of the polyelectrolyte complexation of xanthan and chitosan samples of different degree of polymerization. Biopolymers, 2012, 97, 1-10.	1.2	12
53	Logic swelling response of DNA–polymer hybrid hydrogel. Soft Matter, 2011, 7, 4615.	1.2	38
54	Toehold of dsDNA exchange affects the hydrogel swelling kinetics of a polymer–dsDNA hybrid hydrogel. Soft Matter, 2011, 7, 1741-1746.	1.2	44

#	Article	IF	CITATIONS
55	Higher order structure of short immunostimulatory oligonucleotides studied by atomic force microscopy. Ultramicroscopy, 2010, 110, 689-693.	0.8	23
56	Interferometric characterization of swelling of covalently crosslinked alginate gel and changes associated with polymer impregnation. Carbohydrate Polymers, 2010, 80, 828-832.	5.1	9
57	Alginate Oligoguluronates as a Tool for Tailoring Properties of Caâ€Alginate Gels. Macromolecular Symposia, 2010, 291-292, 345-353.	0.4	10
58	Responsive Hydrogels for Label-Free Signal Transduction within Biosensors. Sensors, 2010, 10, 4381-4409.	2.1	74
59	Singleâ€molecule pair studies of the interactions of the αâ€GalNAc (Tnâ€antigen) form of porcine submaxillary mucin with soybean agglutinin. Biopolymers, 2009, 91, 719-728.	1.2	29
60	Glucose sensors based on a responsive gel incorporated as a Fabry-Perot cavity on a fiber-optic readout platform. Biosensors and Bioelectronics, 2009, 24, 2034-2039.	5.3	87
61	Structure and stability of polynucleotide-(1,3)-β-D-glucan complexes. Carbohydrate Polymers, 2009, 76, 389-399.	5.1	12
62	Single Molecular Pair Interactions between Hydrophobically Modified Hydroxyethyl Cellulose and Amylose Determined by Dynamic Force Spectroscopy. Langmuir, 2009, 25, 10174-10182.	1.6	14
63	Development of an Oligonucleotide Functionalized Hydrogel Integrated on a High Resolution Interferometric Readout Platform as a Label-Free Macromolecule Sensing Device. Biomacromolecules, 2009, 10, 1619-1626.	2.6	43
64	Determination of Glucose Levels Using a Functionalized Hydrogelâ^'Optical Fiber Biosensor: Toward Continuous Monitoring of Blood Glucose in Vivo. Analytical Chemistry, 2009, 81, 3630-3636.	3.2	116
65	Higher order structure of (1,3)â€Î²â€< scp>Dâ€glucans and its influence on their biological activities and complexation abilities. Biopolymers, 2008, 89, 310-321.	1.2	156
66	The fluid phase of morsellized bone: Characterization of viscosity and chemical composition. Journal of the Mechanical Behavior of Biomedical Materials, 2008, 1, 199-205.	1.5	5
67	Polyelectrolyte layer interpenetration and swelling of alginate–chitosan multilayers studied by dual wavelength reflection interference contrast microscopy. Carbohydrate Polymers, 2008, 71, 672-681.	5.1	30
68	Polyelectrolyte complex formation using alginate and chitosan. Carbohydrate Polymers, 2008, 74, 813-821.	5.1	290
69	Quantitative analysis of atomic force microscopy topographs of biopolymer multilayers: Surface structure and polymer assembly modes. Thin Solid Films, 2008, 516, 7770-7776.	0.8	13
70	Potentials of bionanotechnology in the study and manufacturing of self-assembled biopolymer complexes and gels. Food Hydrocolloids, 2008, 22, 2-11.	5.6	7
71	Determination of Swelling of Responsive Gels with Nanometer Resolution. Fiber-Optic Based Platform for Hydrogels as Signal Transducers. Analytical Chemistry, 2008, 80, 5086-5093.	3.2	67
72	Evidence for Egg-Box-Compatible Interactions in Calciumâ^'Alginate Gels from Fiber X-ray Diffraction. Biomacromolecules, 2007, 8, 2098-2103.	2.6	389

#	Article	IF	CITATIONS
73	The Influence of Charge Density of Chitosan in the Compaction of the Polyanions DNA and Xanthan. Biomacromolecules, 2007, 8, 1124-1130.	2.6	41
74	Influence of Oligoguluronates on Alginate Gelation, Kinetics, and Polymer Organization. Biomacromolecules, 2007, 8, 2388-2397.	2.6	71
75	Potentiation of Histamine Release by Microfungal (1→3)- and (1→6)-β-D-Glucans. Basic and Clinical Pharmacology and Toxicology, 2007, 101, 455-458.	1.2	22
76	Determination of Molecular Parameters of Linear and Circular Scleroglucan Coexisting in Ternary Mixtures Using Light Scattering. Biomacromolecules, 2006, 7, 858-865.	2.6	20
77	Similarities and differences between alginic acid gels and ionically crosslinked alginate gels. Food Hydrocolloids, 2006, 20, 170-175.	5.6	130
78	Small angle x-ray scattering study of local structure and collapse transition of (1,3)-β-D-glucan-chitosan gels. Journal of Chemical Physics, 2006, 125, 054908.	1.2	7
79	Electrostatically Self-Assembled Multilayers of Chitosan and Xanthan Studied by Atomic Force Microscopy and Micro-Interferometry. Macromolecular Symposia, 2005, 227, 161-172.	0.4	9
80	Swelling, mechanical properties and effect of annealing of scleroglucan gels. Carbohydrate Polymers, 2005, 60, 363-378.	5.1	2
81	Mapping enzymatic functionalities of mannuronan C-5 epimerases and their modular units by dynamic force spectroscopy. Carbohydrate Research, 2005, 340, 2782-2795.	1.1	16
82	Toroids of stiff polyelectrolytes. Current Opinion in Colloid and Interface Science, 2005, 10, 16-21.	3.4	24
83	DNA-polycation complexation and polyplex stability in the presence of competing polyanions. Biopolymers, 2005, 77, 86-97.	1.2	61
84	Development and application of a model for chitosan hydrolysis by a family 18 chitinase. Biopolymers, 2005, 77, 273-285.	1.2	29
85	Probing macromolecular architectures of nanosized cyclic structures of (1→3)-β-d-glucans by AFM and SEC-MALLS. Carbohydrate Research, 2005, 340, 971-979.	1.1	31
86	Glycosaminoglycan destabilization of DNA–chitosan polyplexes for gene delivery depends on chitosan chain length and GAG properties. Biochimica Et Biophysica Acta - General Subjects, 2005, 1721, 44-54.	1.1	73
87	Biochemical analysis of the processive mechanism for epimerization of alginate by mannuronan C-5 epimerase AlgE4. Biochemical Journal, 2004, 381, 155-164.	1.7	88
88	Improved chitosan-mediated gene delivery based on easily dissociated chitosan polyplexes of highly defined chitosan oligomers. Gene Therapy, 2004, 11, 1441-1452.	2.3	363
89	Metastable and stable states of xanthan polyelectrolyte complexes studied by atomic force microscopy. Biopolymers, 2004, 74, 199-213.	1.2	49
90	Crystal Structure of Cellulose Triacetate I. Macromolecules, 2004, 37, 4547-4553.	2.2	46

#	Article	IF	CITATIONS
91	Single-molecular Pair Unbinding Studies of Mannuronan C-5 Epimerase AlgE4 and Its Polymer Substrate Biomacromolecules, 2004, 5, 1288-1295.	2.6	45
92	Structural Analysis of Chitosan Mediated DNA Condensation by AFM:Â Influence of Chitosan Molecular Parameters. Biomacromolecules, 2004, 5, 928-936.	2.6	128
93	Characterisation of bacterial polysaccharides: steps towards single-molecular studies. Carbohydrate Research, 2003, 338, 2459-2475.	1.1	48
94	Analysis of Compacted Semiflexible Polyanions Visualized by Atomic Force Microscopy:Â Influence of Chain Stiffness on the Morphologies of Polyelectrolyte Complexesâ€. Journal of Physical Chemistry B, 2003, 107, 8172-8180.	1.2	71
95	Scleroglucan Gelation byin SituNeutralization of the Alkaline Solution. Biomacromolecules, 2003, 4, 914-921.	2.6	17
96	Small-Angle X-ray Scattering and Rheological Characterization of Alginate Gels. 3. Alginic Acid Gels. Biomacromolecules, 2003, 4, 1661-1668.	2.6	88
97	Mode of action of recombinantAzotobacter vinelandiimannuronan C-5 epimerases AlgE2 and AlgE4. Biopolymers, 2002, 63, 77-88.	1.2	54
98	Structural stability of (1→3)-β-d-glucan macrocycles. Carbohydrate Polymers, 2001, 44, 113-121.	5.1	26
99	Gelation of periodate oxidised scleroglucan (scleraldehyde). Carbohydrate Polymers, 2001, 46, 241-248.	5.1	21
100	Effects of molecular weight and elastic segment flexibility on syneresis in Ca-alginate gels. Food Hydrocolloids, 2001, 15, 485-490.	5.6	91
101	The cytokine stimulating activity of (1→3)-β-d-glucans is dependent on the triple helix conformation. Carbohydrate Research, 2000, 329, 587-596.	1.1	211
102	Small-angle X-ray scattering and rheological characterization of alginate gels. 2. Time-resolved studies on ionotropic gels. Journal of Molecular Structure, 2000, 554, 21-34.	1.8	49
103	Small-Angle X-ray Scattering and Rheological Characterization of Alginate Gels. 1. Caâ^'Alginate Gels. Macromolecules, 2000, 33, 1853-1863.	2.2	308
104	The Recombinant Azotobacter vinelandii Mannuronan C-5-Epimerase AlgE4 Epimerizes Alginate by a Nonrandom Attack Mechanism. Journal of Biological Chemistry, 1999, 274, 12316-12322.	1.6	79
105	Scleroglucan gel volume changes in dimethylsulphoxide/water and alkaline solutions are partly caused by polymer chain conformational transitions. Carbohydrate Polymers, 1999, 39, 249-255.	5.1	7
106	Mode of action of chitin deacetylase from Mucor rouxii on partially N-acetylated chitosans. Carbohydrate Research, 1998, 311, 71-78.	1.1	53
107	Free-radical degradation of triple-stranded scleroglucan by hydrogen peroxide and ferrous ions. Carbohydrate Polymers, 1998, 37, 41-48.	5.1	28
108	Gelation kinetics of scleraldehyde–chitosan co-gels. Polymer Gels and Networks, 1998, 6, 113-135.	0.6	26

#	Article	IF	CITATIONS
109	Sclerox-chitosan co-gels: Effects of charge density on swelling of gels in ionic aqueous solution and in poor solvents, and on the rehydration of dried gels. Polymer Gels and Networks, 1998, 6, 471-492.	0.6	24
110	Acid Hydrolysis of κ- and ι-Carrageenan in the Disordered and Ordered Conformations: Characterization of Partially Hydrolyzed Samples and Single-Stranded Oligomers Released from the Ordered Structures. Macromolecules, 1998, 31, 1842-1851.	2.2	46
111	Small-angle X-ray scattering and rheological characterization of alginate gels. Macromolecular Symposia, 1997, 120, 91-101.	0.4	21
112	Colloidal gold and colloidal gold labelled wheat germ agglutinin as molecular probes for identification in mucin/chitosan complexes. Carbohydrate Polymers, 1997, 33, 91-99.	5.1	20
113	Metastable, Partially Depolymerized Xanthans and Rearrangements toward Perfectly Matched Duplex Structures. Macromolecules, 1996, 29, 2939-2944.	2.2	10
114	Release of disordered xanthan oligomers upon partial acid hydrolysis of double-stranded xanthan. Food Hydrocolloids, 1996, 10, 83-89.	5.6	21
115	Transient electric birefringence study of rod-like triple-helical polysaccharide schizophyllan. Carbohydrate Polymers, 1996, 29, 277-283.	5.1	2
116	Carboxylation of scleroglucan for controlled crosslinking by heavy metal ions. Carbohydrate Polymers, 1995, 27, 5-11.	5.1	20
117	Sequence specificities for lysozyme depolymerization of partially N-acetylated chitosans. Canadian Journal of Chemistry, 1995, 73, 1972-1981.	0.6	33
118	Conformation dependent depolymerisation kinetics of polysaccharides studied by viscosity measurements. Carbohydrate Polymers, 1994, 24, 265-275.	5.1	54
119	An antitumor, branched (1 → 3)-β-d-glucan from a water extract of fruiting bodies of Cryptoporus volvatus. Carbohydrate Research, 1994, 263, 111-121.	1.1	84
120	Numerical model for alginate block specificity of mannuronate lyase from Haliotis. Carbohydrate Research, 1994, 260, 83-98.	1.1	14
121	The role of side-chains in the Cr3+-induced gelation of xanthan and xylinan (acetan) variants. Carbohydrate Polymers, 1994, 25, 25-29.	5.1	6
122	Pregel cluster formation in gelling polysaccharides visualized by electron microscopy. Polymer Gels and Networks, 1994, 2, 173-190.	0.6	11
123	Conformation of in aqueous solution. International Journal of Biological Macromolecules, 1994, 16, 313-317.	3.6	20
124	P265 the potential of chitosan as mucoadhesive drug carrier: Studies on its interaction with pig gastric mucin on a molecular level. European Journal of Pharmaceutical Sciences, 1994, 2, 185.	1.9	9
125	Influence of Aqueous Solvation on Side Chain-Backbone Interaction in Comblike Branched Bacterial Polysaccharides. Macromolecules, 1994, 27, 1124-1135.	2.2	6
126	Comparison of scanning tunnelling microscopy and transmission electron microscopy image data of a microbial polysaccharide. Ultramicroscopy, 1993, 48, 197-201.	0.8	29

#	Article	IF	CITATIONS
127	Distribution of uronate residues in alginate chains in relation to alginate gelling properties — 2: Enrichment of β-d-mannuronic acid and depletion of α-l-guluronic acid in sol fraction. Carbohydrate Polymers, 1993, 21, 39-46.	5.1	62
128	Predicted influence of monomer sequence distribution and acetylation on the extension of naturally occurring alginates. Carbohydrate Polymers, 1993, 22, 57-66.	5.1	27
129	Macrocyclization of polysaccharides visualized by electron microscopy. International Journal of Biological Macromolecules, 1993, 15, 63-68.	3.6	54
130	Depolymerization of double-stranded xanthan by acid hydrolysis: characterization of partially degraded double strands and single-stranded oligomers released from the ordered structures. Macromolecules, 1993, 26, 6111-6120.	2.2	60
131	Rheology of xanthan and scleroglucan in synthetic seawater. Carbohydrate Polymers, 1992, 17, 209-220.	5.1	37
132	Degradation of multistranded polymers: effects of interstrand stabilization in xanthan and scleroglucan studied by a Monte Carlo method. Macromolecules, 1992, 25, 2209-2214.	2.2	21
133	Gelation of xanthan with trivalent metal ions. Carbohydrate Polymers, 1992, 18, 243-251.	5.1	67
134	Supercoiling in circular triple-helical polysaccharides. Macromolecules, 1991, 24, 6349-6351.	2.2	63
135	Distribution of uronate residues in alginate chains in relation to alginate gelling properties. Macromolecules, 1991, 24, 4637-4645.	2.2	145
136	Optical rotation of dilute aqueous xanthan solutions at elevated hydrostatic pressure. Journal of Applied Polymer Science, 1991, 42, 2063-2071.	1.3	3
137	Long-term storage of xanthan in seawater at elevated temperature: physical dimensions and chemical composition of degradation products. International Journal of Biological Macromolecules, 1989, 11, 137-144.	3.6	10
138	Controlled gelation of xanthan by trivalent chronic ions. Carbohydrate Polymers, 1988, 8, 245-256.	5.1	22
139	The molecular size and shape of xanthan, xylinan, bronchial mucin, alginate, and amylose as revealed by electron microscopy. Carbohydrate Research, 1987, 160, 13-28.	1.1	75
140	Thermal stability and chain conformational studies of xanthan at different ionic strengths. Carbohydrate Polymers, 1987, 7, 421-433.	5.1	24
141	Spectrin, human erythrocyte shapes, and mechanochemical properties. Biophysical Journal, 1986, 49, 319-327.	0.2	40
142	Electron microscopic study of single-and double-stranded xanthan. International Journal of Biological Macromolecules, 1986, 8, 217-225.	3.6	58
143	The human erythrocyte membrane skeleton may be an ionic gel. European Biophysics Journal, 1986, 13, 203-218.	1.2	73
144	The human erythrocyte membrane skeleton may be an ionic gel. III. Micropipette aspiration of unswollen erythrocytes. Journal of Theoretical Biology, 1986, 123, 205-211.	0.8	18

BjÃ,rn T Stokke

#	Article	IF	CITATIONS
145	The molecular basis of erythrocyte shape. Science, 1986, 234, 1217-1223.	6.0	297
146	A computerized low-shear pendulum viscoelastometer, stress-relaxation, shear creep, and dynamic elastic moduli measurements of soft biogels. International Journal of Bio-medical Computing, 1985, 17, 215-226.	0.5	3
147	A practical, high-resolution, microcomputer-based method for the analysis of relaxation data exhibiting multicomponent exponential decays. International Journal of Bio-medical Computing, 1985, 16, 35-57.	0.5	5
148	An electrophoretic device concentrating charged macromolecules to a predetermined final solution volume. Analytical Biochemistry, 1985, 148, 527-532.	1.1	2